AIAA JOURNAL
Vol. 36, No. 1, January 1998

Optimization Method for Educing Variable-Impedance Liner Properties

Willie R. Watson,* Sharon E. Tanner,† and Tony L. Parrott‡
NASA Langley Research Center, Hampton, Virginia 23681-2199

A new approach to educing normal incidence acoustic impedance of nonuniform test specimens in grazing incidence and grazing-flow environments is described. An optimization algorithm is shown to provide an efficient means for searching out an impedance distribution to match the measured acoustic field along the upper wall of a duct opposite the test specimen. The flow duct is allowed to transmit multimodal, nonprogressive acoustic waves in a flow environment; however, only a no-flow environment is discussed. A key feature of the method is the expansion of the impedance function as a piecewise continuous polynomial with undetermined coefficients. The upper wall acoustic pressure is computed numerically as a function of these coefficients by using a finite element method. The Davidon–Fletcher–Powell optimization algorithm is used to educe the normal incidence impedance by determining the values of the undetermined coefficients that minimize the difference between the measured and the numerically computed upper wall pressure. Results show that this more robust method reduces by a factor of 30 the time required to make impedance determinations as compared with the contour deformation method and is better suited for liners with spatially varying impedance.

Nomenclature

$[A(\beta_1^J, \beta_2^J)]$	= complex block-tridiagonal matrices with order MN
c_0, ρ_0	= ambient sound speed and density, respectively
$E(\beta_1^J, \beta_2^J)$	= positive-definite objective function
$\{F\}$	= vector that contains source effects
H, L	= height and length, respectively, of two-dimensional duct
i	= $\sqrt{-1}$
k	= free-space wave number
L_1, L_2	= leading and trailing edge, respectively, of test liner
M, N	= number of nodes in the y and x directions, respectively
m	= number of upper wall measurement points
$P_{\mathrm{FE}}(x_l; \beta_1^J, \beta_2^J)$	= finite element upper wall pressure where x is equal to x_l
$P_{\mathrm{wall}}(x_l)$	= measured upper wall acoustic pressure where x is equal to x_l
$p(x, y)$	= complex acoustic pressure at (x, y)
$p_s(y)$	= measured acoustic pressure at source plane
x, y, z	= Cartesian coordinates
$x_1, x_2, \ldots, x_m$	= axial location of upper wall pressure measurements
β_1^J, β_2^J	= undetermined coefficients for acoustic admittance expansion
$\beta(x)$	= normalized acoustic admittance, $\xi(x) + i\sigma(x)$
$\zeta(x), \zeta_{\mathrm{exit}}(y)$	= normalized wall and exit plane impedance, respectively
$\xi(x), \sigma(x)$	= normalized acoustic conductance and susceptance, respectively
$\{\Phi\}$	= global vector of complex acoustic pressures
$\|\|$	= absolute value of complex quantity

Subscripts

I	= node counter for axial direction
J	= node counter for transverse direction
l	= upper wall measurement point counter
m	= total number of upper wall measurement points

Received March 4, 1997; presented as Paper 97-1704 at the AIAA/CEAS 3rd Aeroacoustics Conference, Atlanta, GA, May 12–14, 1997; revision received Aug. 19, 1997; accepted for publication Aug. 28, 1997.

*Senior Research Scientist, Aerodynamic and Acoustics Methods Branch, Fluid Mechanics and Acoustics Division, Mail Stop 128.

†Research Scientist, Structural Acoustics Branch, Fluid Mechanics and Acoustics Division, Mail Stop 463. Senior Member AIAA.

‡Senior Research Scientist, Structural Acoustics Branch, Fluid Mechanics and Acoustics Division, Mail Stop 463.

Introduction

EFFICIENT duct treatments for broadband acoustic noise suppression remain critical to the development in the next century of environmentally acceptable commercial aircraft. To this end, an accurate knowledge of duct treatment impedance is a critical aspect of duct treatment design. To validate liner impedance prediction models, which must include grazing-flow effects, a flow-duct apparatus is arranged to allow acoustic field measurements to be conducted conveniently under controlled laboratory conditions. From these measurements, the normal incidence impedance in a grazing incidence and grazing flow environment and for locally reacting test materials can, in theory, be educed. Several methods are available for accomplishing this eduction process with varying requirements in terms of experimental and computational effort. Perhaps the simplest approach, the so-called infinite waveguide method, relies on the measurement of an assumed single, unidirectional propagating mode.[1–3] In this case, a modal solution relates the normal incidence impedance of the test specimen to the measured mode propagation constant in the duct. However, in real facilities, sufficiently idealized test conditions, i.e., a single unidirectional propagating mode, are rarely attained. Additionally, if the test liner impedance is nonuniform, i.e., the impedance varies in the lengthwise direction, either by design or because of nonlinear response, added wave field complexity results from energy scatter into higher-order modes. Although this condition may be desirable in achieving more efficient, broadband absorbing structures, it is a complicating feature that cannot be handled by the infinite waveguide method for impedance determination.

In a recent paper, a finite element-based contour deformation method was developed for educing the acoustic impedance of a material installed as a finite length wall segment of a no-flow duct that carried a nonprogressive multimodal sound field.[4] The method was validated for a uniform test specimen; the results agreed well with the normal incidence impedance spectrum as determined at normal incidence in a standing wave tube (SWT).[5] Although the contour

deformation method was shown not to be computationally intense for uniform liners,[5] this conclusion does not hold true for a variable impedance liner. Consider, for example, the time required to obtain the uniform impedance eductions using the DEC Alpha workstation in Ref. 5. Approximately 3400 impedance grid calculations were required to educe the impedance of each uniform liner. Because the CPU time required to perform a calculation at each impedance grid point was approximately 0.5 s, the total CPU time required to educe the uniform liner impedance was approximately 30 CPU min. However, the CPU time required to compute the impedance of a variable impedance liner, i.e., such as a segmented liner, does not scale linearly. For example, a two-segment liner would require 30^2, or 900, CPU min, and a three-segment liner would require 30^3, or 27,000, CPU min. Thus, when the contour deformation method is applied to a variable-impedance liner, the problem becomes computationally intense.

The objective of this paper is to document the results of an efficient optimization algorithm by utilizing a finite element wave-propagation model to educe nonuniform test liner impedance from complex acoustic pressure measurements in a flow-duct environment. Specifically, this paper describes a validation exercise on six uniform and one nonuniform liner structure. The following section describes the mathematical model, governing equations, boundary conditions, and experimental apparatus. The unknown impedance function is expanded as a piecewise continuous polynomial with undetermined coefficients. The undetermined coefficients in the impedance expansion are determined by minimizing an objective function using Stewart's adaptation[6] of the Davidon–Fletcher–Powell (SDFP) optimization algorithm. The optimization algorithm is discussed in the "Impedance Eduction Method" section. The SDFP method replaces the contour deformation method that was developed in the original paper.[4] The liner configurations tested and the supporting normal incidence impedance tests that were conducted are described in the section entitled "Description of Test Liners." In the Results section, impedances educed by means of the SDFP method are compared with values obtained with normal incidence measurements. Conclusions and ongoing research activities are discussed in the final section.

Problem Formulation

The test-liner-specific measured data that are required as input to the SDFP method are complex acoustic pressure measurements (amplitude and phase), which are taken along the upper wall at a location opposite the test specimen. Other input data needed are the source-plane pressure and the exit-plane impedance. These data are obtained in the NASA Langley Research Center flow impedance facility. The 51-mm-square cross section part of this facility is shown in Fig. 1. A complete description of the components of the apparatus is given in detail elsewhere.[5] In this validation exercise, excitation frequencies are limited such that no higher-order modes propagate in the hard-wall section. The test-liner-specific data and source-plane data are taken by a single, flush-mounted traversing microphone mounted on the upper wall as shown in Fig. 1. The exit-plane impedance is determined by implementing the standard two-microphone method about 1 m downstream of the test liner trailing edge.[7] Figure 2 shows the two-dimensional no-flow duct that is used to model the test section part of the facility. Throughout this

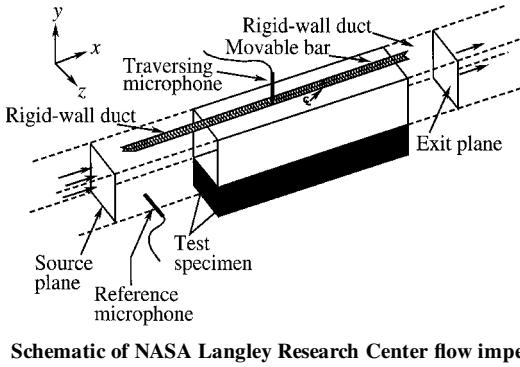

Fig. 1 Schematic of NASA Langley Research Center flow impedance tube.

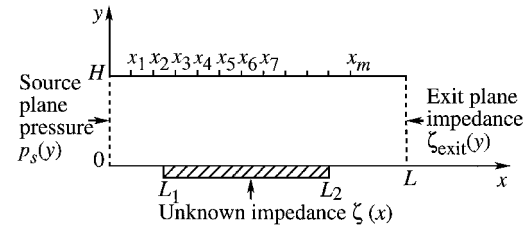

Fig. 2 Modeled portion of NASA Langley Research Center flow impedance tube and coordinate system.

work, all impedances are normalized with respect to the characteristic impedance of the air in the duct, i.e., $\rho_0 c_0$. The upper wall of the duct is rigid, and m points are designated at $x = x_1, x_2, x_3, \ldots, x_m$ along the rigid upper wall, at which complex acoustic pressures are measured that are to be matched by the SDFP procedure.

The test liner forms the bottom wall of the duct between the leading-edge location L_1 and the trailing-edge location L_2, i.e., a distance of about 406 mm. Although all test liners are assumed to be locally reacting, they may have a nonuniform impedance distribution in the lengthwise direction given by $\zeta(x)$, as shown. The task of the SDFP method is to find $\zeta(x)$ such that the predicted upper wall acoustic pressure distribution reproduces that measured by the flush-mounted traversing microphone (Fig. 1). Note (see Fig. 1) that the mathematical model discussed here is limited to a two-dimensional description that approximates the three-dimensional flow impedance tube shown. This two-dimensional model is adequate provided that the frequency is sufficiently low to ensure constancy of the acoustic field with z, as shown in Fig. 1.

The mathematical problem is to find (by using $e^{i\omega t}$ time convention) the solution to the Helmholtz equation

$$\frac{\partial^2 p(x, y)}{\partial x^2} + \frac{\partial^2 p(x, y)}{\partial y^2} + k^2 p(x, y) = 0 \tag{1}$$

Along the source plane of the duct, the acoustic boundary condition is

$$p(0, y) = p_s(y) \tag{2}$$

The boundary condition along the rigid upper wall is equivalent to the requirement that the gradient of acoustic pressure normal to the wall must vanish:

$$\frac{\partial p(x, H)}{\partial y} = 0 \tag{3}$$

At the duct termination, the ratio of acoustic pressure to the axial velocity must equal the measured exit impedance:

$$\frac{\partial p(L, y)}{\partial x} = \frac{-ikp(L, y)}{\zeta_{exit}(y)} \tag{4}$$

Finally, the acoustic material is assumed to be locally reacting, so that the lower wall boundary condition is expressed in terms of the acoustic admittance:

$$\frac{\partial p(x, 0)}{\partial y} = ik\beta(x)p(x, 0) \tag{5}$$

$$\beta(x) = 1/\zeta(x) = \xi(x) + i\sigma(x) \tag{6}$$

where the conductance $\xi(x)$ and the susceptance $\sigma(x)$ are functions to be determined. Equations (1–5) form a well-posed boundary value problem that can be solved numerically to determine uniquely the upper wall pressures for given conductance and susceptance functions. Conversely, unique conductance and susceptance functions exist that will reproduce the measured upper wall pressure. The goal here is to devise a procedure for educing these unknown functions.

Impedance Eduction Method

The method chosen to obtain the upper wall pressures for specified conductance and susceptance functions parallels that discussed in Ref. 4; sufficient detail is presented here only to highlight the differences between the two impedance eduction techniques. To begin, upper wall pressures are computed numerically by using a Galerkin finite element method with integration by parts to incorporate the

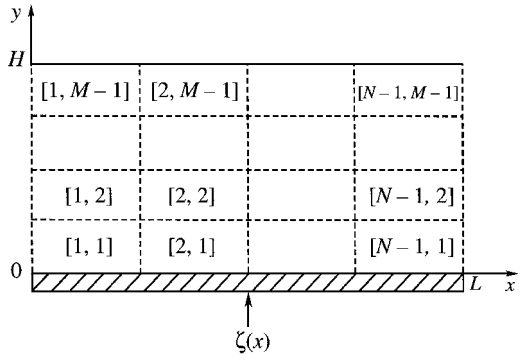

Fig. 3 Finite element discretization of two-dimensional duct.

admittance boundary condition. Linear basis functions are used to expand the acoustic pressure field; N nodes are assumed in the axial direction, and M nodes are assumed in the transverse direction of the duct, as shown in Fig. 3. Within each of the $(N-1)$ lower wall elements, the admittance function is expanded as a piecewise linear function with two undetermined coefficients β_1^J and β_2^J for each element J:

$$\beta(x) = \left[1 - \frac{(x - x_J)}{(x_{J+1} - x_J)}\right]\beta_1^J + \frac{(x - x_J)}{(x_{J+1} - x_J)}\beta_2^J \qquad (7)$$

so that generally $2(N-1)$ unknowns exist. By assembling the elements for the entire domain and applying the sound source condition, a matrix equation is obtained of the form

$$\left[A\left(\beta_1^J, \beta_2^J\right)\right]\{\Phi\} = \{F\} \qquad (8)$$

The solution to Eq. (8) yields the solution to the upper wall pressure as a function of β_1^J and β_2^J.

The unknown coefficients β_1^J and β_2^J of the admittance expansion are determined from the measured upper wall acoustic pressures. The procedure is to determine values of these coefficients such that the upper wall pressure solution obtained from Eq. (8) reproduces the measured value. These values are achieved by minimizing the objective function

$$E\left(\beta_1^J, \beta_2^J\right) = \sum_{l=1}^{m} \left| P_{\text{wall}}(x_l) - P_{\text{FE}}\left(x_l; \beta_1^J, \beta_2^J\right)\right| \qquad (9)$$

Note that the positive-definite objective function may be interpreted as the absolute value of the difference between the measured acoustic wall pressure and that computed by the finite element method.

Because the optimization algorithm makes use of the objective function gradient to find its minimum and this function is available only in numerical form, i.e., as a finite element solution of Eq. (8), we use the SDFP optimization method.[6] The two major features of the SDFP method are the use of a finite difference approximation to the gradient and repeated parabolic interpolation to determine values of the optimization variables that minimize the objective function.

Description of Test Liners

The impedances of seven liners are determined by using the SDFP approach. The normal incidence impedance of each liner structure is measured in a normal incidence impedance tube using the two-microphone method for impedance measurement.[7] Six of these liners have a uniform impedance distribution. Only the seventh has a nonuniform impedance distribution, which is achieved by three stepped changes in the liner cavity depth. The seven liners, shown schematically in Fig. 4, are described further.

1) Liner a (Fig. 4) is actually a stainless steel insert that continues the hard-wall condition of the flow duct. The liner is used to provide a baseline condition for establishing zero admittance.

2) Liner b (Fig. 4) consists of a ceramic structure of parallel, cylindrical channels, 1 mm in diameter, embedded in a ceramic matrix. The channels, 76 mm deep, run perpendicular to the exposed surface to provide a surface porosity of 57%. The channels are rigidly terminated such that each is isolated from its neighbor to ensure a locally reacting structure. This material is useful only as a calibration liner in laboratory experiments because of its predictable and consistent acoustic properties; however, its weight and brittleness make it unrealistic for aircraft applications.

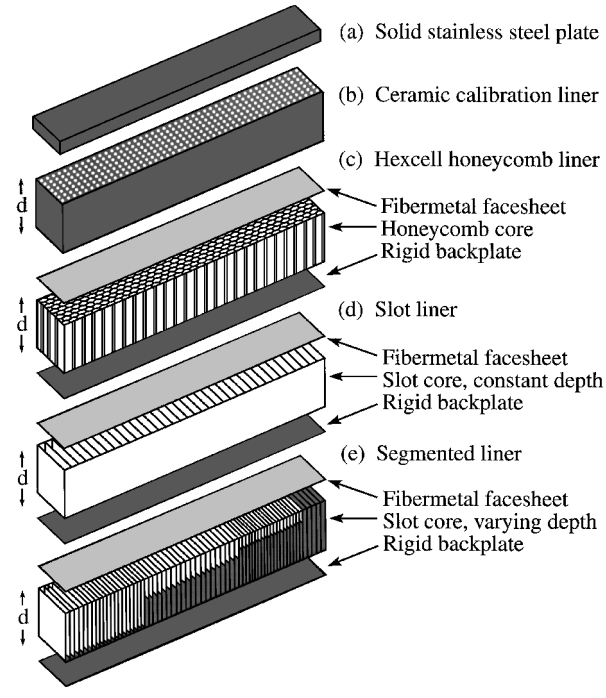

Fig. 4 Schematic of liner test bed.

3) Liner c (Fig. 4) is a conventional hexcell honeycomb liner, which is representative of that currently used in commercial aircraft engines. This liner is composed of hexcell honeycomb material (each cell is 6 mm in diameter) with a 100-mks rayl fibermetal facesheet bonded to the honeycomb surface. The total depth of this test liner is 101 mm.

4) Three slot liner configurations (d in Fig. 4) are used, each composed of 65 slot cavities of uniform depth. The basic test liner is 76 mm deep and consists of 66 aluminum parallel plates that are placed approximately 6 mm apart. A 100-mks rayl fibermetal facesheet is bonded to the surface of the liner. The slot-liner impedance is educed with SDFP in the basic configuration (76-mm depth) and for two shallower depths, i.e., 38 and 25 mm. To modify the depth of the liner, snug-fitting Plexiglas® inserts are placed in each slot to achieve the desired depths.

5) The final test liner (e in Fig. 4) is segmented into three equal parts, which are constructed by combining three slot-liner segments with depths of 76, 38, and 25 mm in series, as shown. Each segment contains 20 slots, and the remaining five slots near the trailing edge of the segmented liner are deactivated by inserting full-length Plexiglas plugs. The depths are such that the resonant frequencies of the second and third segments are first and second harmonics of the first segment resonance. In the SDFP prediction program, the impedance of each segment of the segmented liner is assumed to be constant, and the five slots near the trailing edge are set to hard-wall impedance values. Because each segment of the variable-impedance slot liner is locally reacting, the known impedance of each segment will be the impedance established as described in item 4.

Each test specimen spans the width of the impedance tube. Note that the experimentally determined, normal incidence impedances for the three uniform slot liners are prone to somewhat more systematic error than are the ceramic and hexcell honeycomb liners. This possible loss of accuracy is attributable either to the fact that the 51 mm width of the SWT apparatus is not precisely equal to a multiple of the slot width or to the less than perfect mounting procedure that may not provide as airtight a seal as was provided for the custom made test sample holders for the SWT apparatus.

Results

An in-house computer code that implements the SDFP impedance eduction, or measurement, method has been developed. Solution of

the finite element matrix equation and minimization of the objective function are performed by using highly developed software packages that are available at NASA Langley Research Center. The undetermined coefficients β_1^J and β_2^J are returned by the SDFP optimization algorithm. These coefficients are then substituted into the admittance expansion in each lower wall element to determine the conductance function $\xi(x)$ and the susceptance function $\sigma(x)$ that are consistent with the measured acoustic pressure distribution on the upper wall. Results are computed with a DEC Alpha workstation. An evenly spaced 231×21 grid is used ($N = 231$ and $M = 21$) in the finite element discretization for all calculations. This grid ensures that a minimum of 10 elements per axial wavelength is used in the finite element discretization at the highest frequency of interest. To limit the number of optimization variables, all uniform liner studies are performed with only two optimization variables: ξ and σ, i.e., $\beta_1^J = \beta_2^J = \xi + i\sigma$. Segmented-liner studies are performed in a similar manner; however, six optimization variables are used, i.e., a conductance and susceptance variable for each liner segment.

Figure 5 shows the SDFP-educed conductance spectrum for the hard-wall, ceramic, and hexcell honeycomb liners. Educed values of conductance for the hard-wall liner are in excellent agreement with the known values of a solid surface, i.e., conductances for a nonconducting solid surface are zero. Comparisons between the SDFP-educed conductance values and those measured for the two soft surfaces, i.e., the ceramic and hexcell honeycomb liners, agree well, except at the frequency closest to the resonant frequency, i.e., 1000 Hz, of the ceramic material. For highly tuned liners at resonance, a decrease is generally noted in the accuracy of the measured data as a result of a signal-to-noise problem. This decrease in accuracy probably accounts for the discrepancy near the resonance frequency of the ceramic liner. The susceptance plots are shown in Fig. 6. Note that the SDFP-educed susceptance of the hard-wall liner agrees well with the known values (the susceptance for a rigid surface is zero). The educed susceptance values for the soft surfaces agree well with the measured values, except at the resonant frequency of the ceramic material (1000 Hz) and the resonant frequency of the hexcell honeycomb material (2500 Hz).

Note also that the accuracies of the impedance eductions for each of the uniform liners in Figs. 5 and 6 are comparable to the accuracy obtained with the contour deformation method, i.e., two significant digits of accuracy, except at the resonant frequency. However, the contour deformation method[5] requires a CPU time of 30 min per frequency, whereas the SDFP method requires only 50 s of CPU time per frequency on the same workstation. Thus, the SDFP method was able to educe the unknown impedance to the same accuracy as the contour deformation method but at a fraction of the required CPU time.

Figure 7 shows comparisons between the measured conductance and that determined by the SDFP method for each of the three

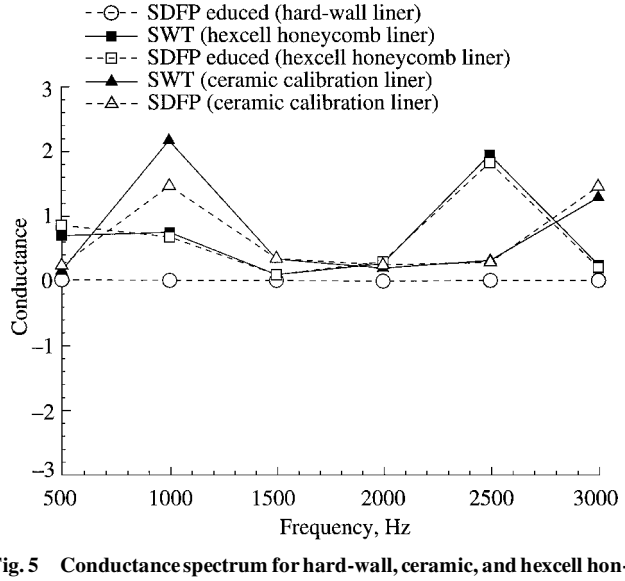

Fig. 5 Conductance spectrum for hard-wall, ceramic, and hexcell honeycomb liner.

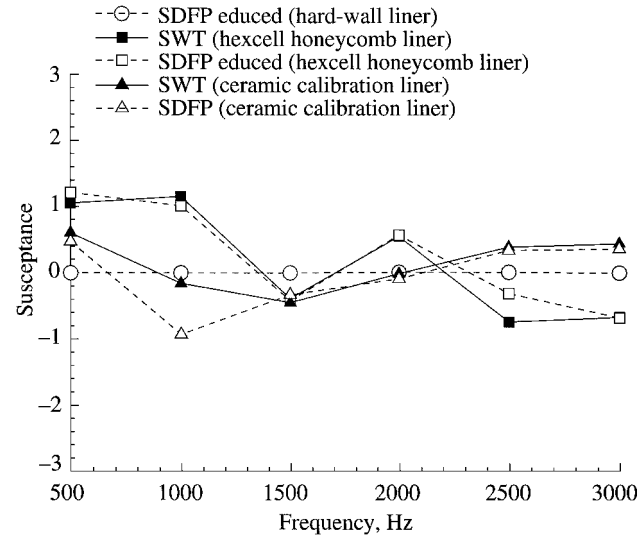

Fig. 6 Susceptance spectrum for hard-wall, ceramic, and hexcell honeycomb liner.

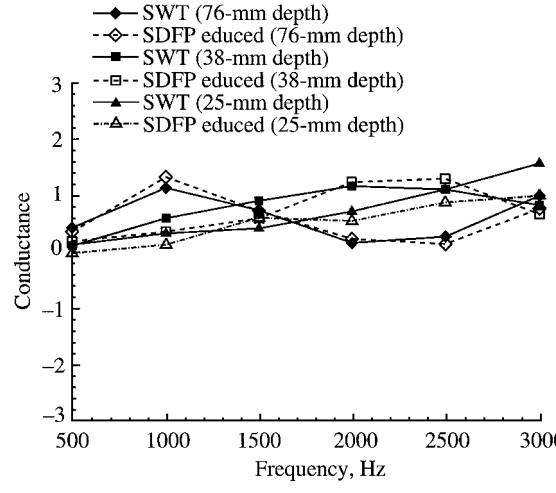

Fig. 7 Conductance spectrum for three slot-liner depths.

uniform-depth slot liners. The agreement is good, although the comparisons are not as close as those for the ceramic and hexcell honeycomb liners. The reader is reminded that the measurements shown in Fig. 7 are more subject to systematic error than the measurements obtained for the ceramic and hexcell honeycomb liners. The SDFP-educed conductances for the slot liner with the greatest depth (76 mm) are in good agreement with measured values, except near the two resonant frequencies of the slot liner, i.e., 1000 and 3000 Hz. Note that this slot liner contains no Plexiglas inserts. A loss of accuracy is generally noted in the eductions of the conductance as the percentage of the cavities that is filled with Plexiglas increases. Specifically, SDFP-educed and measured conductance values do not compare as well for the slot liner with a depth of 25 mm. Measured and SDFP-educed conductance values compare better at the lower frequencies. Note the large discrepancy at the resonant frequency (3000 Hz) of the slot liner with a depth of 25 mm. Comparisons of educed and measured susceptance values for the uniform slot liners are shown in Fig. 8. The agreement between the measured and SDFP-educed susceptance values is better than for the conductance values. The largest discrepancy between the measured and the SDFP-educed susceptance spectrum occurs near the resonant frequencies (1000 and 3000 Hz) for the slot liner with a depth of 76 mm.

An appropriate next step in the validation of the SDFP method is to show that the method can educe the impedance of each segment in a segmented liner. Segmented-liner properties are not measurable in a normal incidence impedance tube, although some success has been achieved in predicting a smeared, or average, value.[8] Figure 9

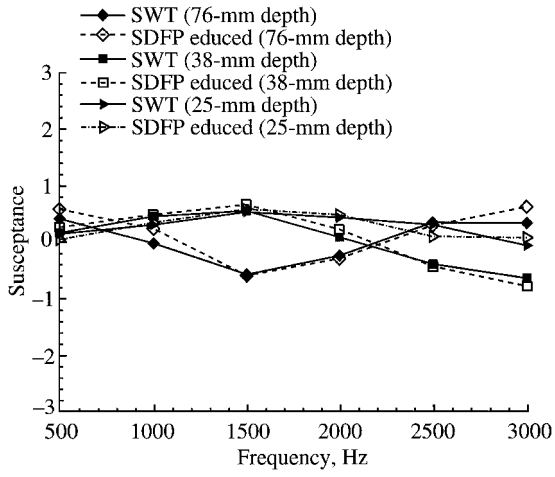

Fig. 8 Susceptance spectrum for three slot-liner depths.

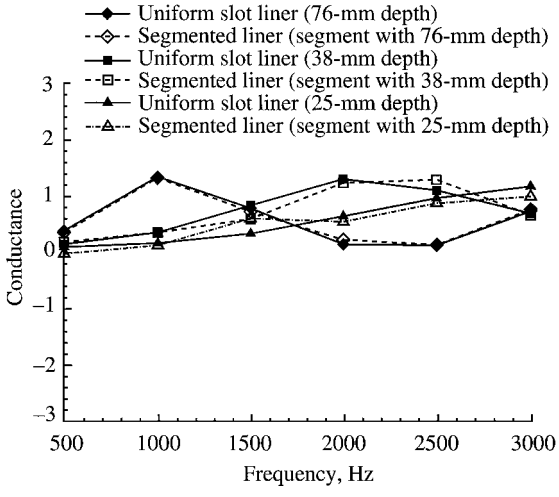

Fig. 9 SDFP-educed conductance spectrum for uniform and segmented liner.

shows the SDFP-educed conductances of the three segments of the segmented liner. The SDFP results obtained for the full-length uniform counterpart, i.e., the 406-mm uniform slot liner, are used as a baseline for comparison. The agreement between the baseline values of the segment with a 76-mm depth, i.e., no Plexiglas inserts, is excellent. Good agreement for the segment with a depth of 38 mm is also obtained. The agreement for the segment with a 25-mm depth is acceptable, although the agreement is not as good as for the segment with a depth of 76 mm. Note that the segment with the smallest depth is connected to a Plexiglas plug that is 32 mm long, for which the admittance is assumed to be zero in the predictive code. The fact that Plexiglas is not a perfectly rigid surface may account for the slight drop in the accuracy of the prediction for the third segment. Comparisons between the measured and the educed susceptance values are shown in Fig. 10. The trends shown here are consistent with those evident in the conductance plots, i.e., a slight loss is noted in the accuracy of the comparisons for the segment with a depth of 25 mm.

The sensitivity of the educed impedance values to random error in the measured data may affect any conclusion reached in this paper. Recall that the effects on the educed impedance of a random error range of ± 0.1 dB in the measurement system have been evaluated in a previous paper.[4] The ± 0.1-dB random error range was not arbitrarily chosen but is, in fact, typical of that found in the NASA Langley Research Center grazing flow impedance tube facility. A random error in this range has been shown to have little effect on the educed impedance spectrum.[4] Although this paper includes a variable-impedance spectrum and uses an optimization algorithm to educe the impedance of the liner, the same conclusion in regards to this random error is expected. This same conclusion is expected

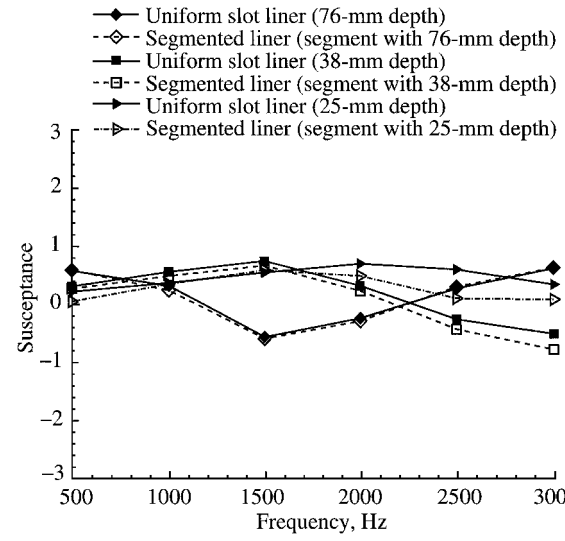

Fig. 10 SDFP-educed susceptance spectrum for uniform and segmented liner.

because the variable impedance does not change the random error in the measurement system, and the optimization method uses the same method to solve Eq. (8).

Conclusions

Based on the results of this work, the following specific conclusions are drawn.

1) The development of the Davidon–Fletcher–Powell optimization algorithm for impedance eduction (SDFP) represents a significant step forward in impedance measurement technology.

2) The SDFP method reduces the time required to make impedance eductions by a factor of 30 in comparison with the contour deformation method and is better suited to variable-impedance liner structures.

3) The SDFP impedance eduction method reproduces measured normal incidence impedance spectra for each uniform liner structure in a liner test bed, except at the resonant frequencies where the quality of the measured data is known to be poor.

4) The SDFP impedance eduction method reproduces the known impedance of each segment within a segmented liner. Future validation studies should not assume a zero admittance for the Plexiglas but should allow the optimization algorithm to determine the admittance of the Plexiglas.

Note that efforts are underway to test this method on continuously varying liner structures.

Although this paper develops the impedance eduction method in an environment without flow, the ultimate goal of the research is to include the effects of high-speed grazing flow. The major challenge in a flow environment is to provide sufficiently accurate boundary condition data at the source and exit planes such as that prescribed by Eqs. (2) and (4). Recall that in the source plane of a flow duct both the complex acoustic pressure distribution and the entrance impedance are required, whereas in the exit plane only the exit impedance distribution is required. Presumably, the successful measurement of the complex pressures at two closely spaced planes would permit acoustic particle velocities to be inferred, thus permitting calculation of the exit or entrance-plane impedance. Although fraught with difficulty, this approach is being actively pursued through the development of inflow acoustic probes to directly measure acoustic pressure distributions in both the source and exit planes. A second approach for acquiring source and exit plane data is also being pursued. In this approach, acoustic pressure measurements are confined entirely to walls of the source and exit sections of the flow duct. These pressure measurements are then used to construct the inflow pressure and particle velocity fields from a modal decomposition of the wall pressure measurements. The advantages of this approach are 1) the avoidance of inflow measurements and 2) the intuitive appeal and physical insight that is provided by the modal propagation model.

Acknowledgment

The authors wish to express their appreciation to M. G. Jones of the Lockheed Martin Corporation for his valuable service in the laboratory phase of this research.

References

[1]Armstrong, D. L., and Olsen, R. F., "Impedance Measurements of Acoustic Duct Liners with Grazing Flow," 87th Meeting of the Acoustical Society of America, New York, April 1974.

[2]Watson, W. R., "A Method for Determining Acoustic-Liner Admittance in a Rectangular Duct with Grazing Flow from Experimental Data," NASA TP-2310, July 1984.

[3]Watson, W. R., "A New Method for Determining Acoustic-Liner Admittance in Ducts with Sheared Flow in Two Cross-Sectional Directions," NASA TP-2518, Oct. 1985.

[4]Watson, W. R., Tanner, S. E., and Parrott, T. L., "A Finite Element Model for Extracting Normal Incidence Impedance in Nonprogressive Acoustic Wave Fields," *Journal of Computational Physics*, Vol. 125, April 1996, pp. 177–186.

[5]Watson, W. R., Tanner, S. E., and Parrott, T. L., "Validation of a Numerical Method for Extracting Liner Impedance," *AIAA Journal*, Vol. 34, No. 3, 1996, pp. 548–554.

[6]Stewart, G. W., III, "A Modification of Davidon's Minimization Method to Accept Difference Approximations of Derivatives," *Journal of the ACM*, Vol. 14, No. 1, 1967, pp. 72–83.

[7]Jones, M. G., and Parrott, T. L., "Evaluation of a Multi-Point Method for Determining Acoustic Impedance," *Mechanical Systems and Signal Processing Journal*, Vol. 3, No. 1, 1989, pp. 15–35.

[8]Parrott, T. L., and Jones, M. G., "Parallel-Element Liner Impedances for Improved Absorption of Broadband Sound in Ducts," *Noise Control Engineering Journal*, Vol. 43, No. 6, 1995, pp. 183–195.

S. Glegg
Associate Editor